Towards the Development of Fractional-Order Flight Controllers for the Quadrotor

Wei Dong[1,2], Jie Chen[1], Jiteng Yang[3], Xinjun Sheng[1(✉)], and Xiangyang Zhu[1]

[1] State Key Laboratory of Mechanical System and Vibration, School of Mechanical Engineering, Shanghai Jiaotong University, Shanghai 200240, China
xjsheng@sjtu.edu.cn

[2] State Key Laboratory of Fluid Power and Mechatronic Systems, Zhejiang University, Zhejiang 310058, China

[3] Department of Precision Instrument, Tsinghua University, Beijing 100084, China

Abstract. The criterion for the development and associated parameter tunning of a class of fractional-order proportional-integral-derivative controllers, regarding the attitude stabilization as the inner control loop, is proposed for the quadrotor in this work. To facilitate this development, the dynamic model of the quadrotor is firstly formulated, and the transfer function of the inner loop is presented based on the real-time flights conducted in previous researches. With the obtained transfer function model, a class of fractional order controllers, including fractional order proportional-derivative controllers and proportional-integral controllers are developed accordingly. For each controller, the parameter tunning methods are addressed in details. To verify the effectiveness of this development, numeric simulations are conducted at last, and the results clearly verify the superiority of the fractional order controllers over conventional proportional-integral-derivative controllers in real-time flight of the quadrotor.

Keywords: Quadrotor · Fractional order controller · Paramter tunning · Flight control

1 Introduction

The agilities and versatilities of the quadrotor attract lots of researchers in recent years [1–4]. In this progress, to enhance the performance of the quadrotor, the flight control, trajectory generation and simultaneous localization and mapping are extensively studied [5–9]. In particular, the flight control is the basic but indispensable element for the quadrotor to fulfill their specific missions in real world.

Numbers of well developed flight controllers, such as linear quadratic (LQ) controller [5], sliding-mode controller [10], linear matrix inequalities (LMI) based controller [11] and disturbance observer based controller [12], were proposed during the last decade. Those controllers have effectively improve the performance of the quadrotor in real-time flights. Unfortunately, the dominant flight controller

N. Kubota et al. (Eds.): ICIRA 2016, Part I, LNAI 9834, pp. 63–74, 2016.
DOI: 10.1007/978-3-319-43506-0_6

of the quadrotor is still the classical proportional-integral-derivative (PID) controller [13,14]. This is because with its three-term functionality covering treatment to both transient and steady-state responses, the PID control provides the a simple and efficient solution for real world applications. However, the pure PID technique shows limited capabilities in disturbance rejection [12], which is the main reason that researchers insistently pursue alternative control strategies. Considering those facts, numbers of studies have tried to directly improve the performance of the flight control based on the PID technique. According to those studies, two methods demonstrate promising capabilities. The first one introduces the tracking differentiator, extended state observer, and utilizes the nonlinear proportional-derivative control to improve the performance of the flight control [15]. The second one directly introduces the fractional calculus into the proportional-integral-derivative technique [16].

Comparatively speaking, the second one provides a more explicit solution, which is similar to its traditional counterpart, i.e., the PID controller. In addition, the fractional calculus, with integrals and derivatives of real order instead of integer order, can be properly further utilized in modeling, which is a significantly more comprehensive description for the specific objects, e.g., the quadrotor in this work. This is because objects, such as the quadrotor controlled by this work, might be of fractional order. Therefore, the results may improve the effectiveness of the simulation compared to the traditional methods. In such a case, it will be also logically more suitable to utilize the fractional order controllers (FOCs) to control those objects [16].

FOCs have showed promising capabilities in many applications that suffer from the classical problems of overshoot and resonance, as well as time diffuse applications such as thermal dissipation and chemical mixing [16,17]. The FOCs could better handle the tracking process with a fractional order calculator, as it provides a powerful instrument for the description of memory and hereditary effects in various substance [16]. Therefore, better robustness and stabilities could be achieved with the FOCs.

In view of the state-of-the-art, this work is motivated to develop a class of FOCs and the associated parameter tunning methods for the quadrotor to enhance its robustness. To facilitate this development, the dynamics model of the quadrotor is firstly formulated, and the transfer function of the attitude is presented based on the previous researches. With the transfer function model, a class of FOCs, including PD^{μ}, FO (PD), PI^{λ}, and FO (PI) controllers are developed. For each controller, the parameter tunning methods are addressed in details. To verify the effectiveness of this development, extensive numeric simulations are conducted at last.

The reminder of this paper is organized as follows. First, the Quadrotor dynamics is introduced, and a transfer function is properly adopted to describe the attitude control loop in Sect. 2. Then the stabilized attitude is treated as the pseudo control input of the position control loop, and the design criterion for the FOCs is presented in Sect. 3. In Sect. 4, numeric simulations are provided to verify the effectiveness of the developed FOCs. At last, Sect. 5 concludes this work.

2 Quadrotor Dynamics

To facilitate the following development, the dynamic model of the quadrotor is firstly presented in this section. With this model, the pseudo control variables for the translational flight control are determined, and a first order time-delay transfer function is adopted according to real-time experiments in previous researches.

2.1 Rigid Body Dynamics

The free body diagram and coordinate frames of the quadrotor are shown in Fig. 1. Based on this illustration, four control inputs can be defined as $U_1 = F_1+F_2+F_3+F_4$, $U_2 = (F_2-F_4)L$, $U_3 = (F_3-F_1)L$, $U_4 = M_1-M_2+M_3-M_4$. where L is the length from the rotor to the center of the mass of the quadrotor, and F_i and M_i are the thrust and torque generated by rotor i ($i \in \{1,\ 2,\ 3,\ 4\}$).

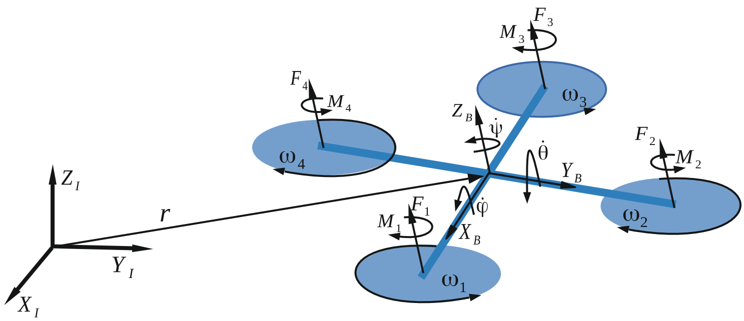

Fig. 1. Free body diagram

In the near hovering state ($\phi \approx 0,\ \theta \approx 0$), the dynamical model of the quadrotor with respect to the inertial coordinates can be then expressed as [7]

$$\begin{aligned} &\ddot{x} = \tfrac{U_1}{m}(\theta\cos\psi + \phi\sin\psi), \quad \ddot{y} = \tfrac{U_1}{m}(\theta\sin\psi - \phi\cos\psi), \\ &\ddot{z} = \tfrac{1}{m}U_1 - g, \quad \ddot{\phi} = \tfrac{U_2}{I_{xx}}, \quad \ddot{\theta} = \tfrac{U_3}{I_{yy}}, \quad \ddot{\psi} = \tfrac{U_4}{I_{zz}}. \end{aligned} \tag{1}$$

where ϕ, θ, and ψ are roll, pitch and yaw, respectively; x, y, and z are the position of the quadrotor in the inertial coordinates; m, I_{xx}, I_{yy}, and I_{zz} are the mass and moments of inertia of the quadrotor, respectively; and g is the gravity constant.

In this way, z, ϕ, θ, and ψ are linearly related to U_i ($i \in \{1,\ 2,\ 3,\ 4\}$). The roll and pitch angle can be then taken as the pseudo control inputs to stabilize x and y. The desired attitude angles can be then explicitly calculated with given translational accelerations as follows

$$\ddot{\boldsymbol{\eta}}^* \triangleq \begin{bmatrix} \theta^* \\ \phi^* \end{bmatrix} = \left(\frac{U_1}{m}\boldsymbol{G}\right)^{-1} \begin{bmatrix} \ddot{x}^* \\ \ddot{y}^* \end{bmatrix} = \frac{m}{U_1}\boldsymbol{G} \begin{bmatrix} \ddot{x}^* \\ \ddot{y}^* \end{bmatrix} \tag{2}$$

where θ^*, ϕ^*, $\ddot{x}^*$, and $\ddot{y}^*$ denote the desired values for θ, ϕ, $\ddot{x}$, and $\ddot{y}$ respectively.

2.2 Dynamics of the Pseudo Control Variables

The pseudo control variables $\boldsymbol{\eta} = [\theta,\ \phi]^T$ utilized in Eq. (2), are commonly stabilized by a inner-loop controller, such as the proportional-derivative (PD) controller [12]. In such a case, real-time experimental identification approaches can be adopted to determine the transfer function from $\boldsymbol{\eta}^*$ to $\boldsymbol{\eta}$, which could be presented in the form of $P_a(s) \approx \frac{1}{Ts+1}\mathrm{e}^{-\tau s}$ [18].

In the near-hovering state, $\frac{U_1}{m}\boldsymbol{G}$ can be treated as a constant, therefore integrating (2) and substituting it into $P_a(s)$, the transfer function taking the attitude command as input and the speed as the output is $P(s) = \frac{K}{s(Ts+1)}\mathrm{e}^{-Ls}$.

The parameters in this transfer function could be identified from series of random flights, which has been addressed in details in [18]. In this work, the following parametric model is adopted

$$P(s) = \frac{1.4}{s(0.05s+1)}\mathrm{e}^{-0.15s} \tag{3}$$

3 Fractional Order Controller Design

Four types of FOCs, namely PD^μ, FO(PD), PI^λ, and FO(PI) controllers are investigated in this section. Based on the model presented in Eq. (3), the criterion for the development of those FOCs is addressed in details.

3.1 PD^μ Controller Development

The PD^μ controller is commonly designed in the following form [17]

$$C(s) = K_p(1 + K_d s^\mu) \tag{4}$$

The PD^μ FOC described by Eq. (4) can be rewritten as

$$C(j\omega) = K_p[(1 + K_d\omega^\mu \cos\frac{\mu\pi}{2}) + jK_d\omega^\mu \sin\frac{\mu\pi}{2}] \tag{5}$$

considering the fact $(j\omega)^\mu = \omega^\mu(\cos\frac{\mu\pi}{2} + i\sin\frac{\mu\pi}{2})$ [19].

The phase and gain of Eq. (5) are

$$\arg[C(j\omega)] = \tan^{-1}\frac{\sin\frac{(1-\mu)\pi}{2} + K_d\omega^\mu}{\cos\frac{(1-\mu)\pi}{2}} - \frac{(1-\mu)\pi}{2} \tag{6}$$

$$|C(j\omega)| = K_p\sqrt{(1 + K_d\omega^u \cos\frac{\mu\pi}{2})^2 + (K_d\omega^\mu \sin\frac{\mu\pi}{2})^2} \tag{7}$$

Similarly, the phase and gain of the original system, i.e., Eq. (3), are

$$\arg[P(j\omega)] = -\tan^{-1}(\omega T) - \frac{\pi}{2} - \omega L,\ |P(j\omega)| = \frac{K}{\omega\sqrt{1 + (\omega T)^2}} \tag{8}$$

The phase and gain of the open-loop $G(s) = C(s)P(s)$ are

$$\arg[G(j\omega)] = \tan^{-1}\frac{\sin\frac{(1-\mu)\pi}{2} + K_d\omega^\mu}{\cos\frac{(1-\mu)\pi}{2}} + \frac{\mu\pi}{2} - \tan^{-1}(\omega T) - \pi - \omega L \qquad (9)$$

$$|G(j\omega)| = \frac{K_p K}{\omega}\sqrt{\frac{(1 + K_d\omega^u\cos\frac{\mu\pi}{2})^2 + (K_d\omega^\mu\sin\frac{\mu\pi}{2})^2}{1 + (\omega T)^2}} \qquad (10)$$

Similar to [20, 21], three specifications are interested by this work in the design of the FOC PD^μ controller. These specifications are proposed as follows:

(i) Proper phase margin ϕ_m should be achieved at $\omega = \omega_c$, i.e., $\arg[G(j\omega)]_{\omega=\omega_c} = -\pi + \phi_m$.
(ii) To guarantee the robustness to the variation in the gain of the plant, the following specification is imposed $\frac{\mathrm{d}(\arg[G(j\omega]))}{\mathrm{d}\omega}|_{\omega=\omega_c} = 0$
(iii) The gain at crossover frequency should be $|G(j\omega_c)|_{dB} = 0$

According to specification (i), the relationship between K_d and μ can be estimated as [17]

$$K_d = \frac{1}{\omega_c^\mu}\tan[\phi_m + \tan^{-1}(\omega_c T) - \frac{\mu\pi}{2} + \omega_c L]\cos\frac{(1-\mu)\pi}{2} - \frac{1}{\omega_c^\mu}\sin\frac{(1-\mu)\pi}{2} \quad (11)$$

To meet the specification (ii) about the robustness to gain variation, one can obtain

$$A\omega_c^{2\mu}K_d^2 + BK_d + A = 0 \qquad (12)$$

which is equivalent to

$$K_d = \frac{-B \pm \sqrt{B^2 - 4A^2\omega_c^{2\mu}}}{2A\omega_c^{2\mu}} \qquad (13)$$

where $B = 2A\omega_c^\mu\sin\frac{(1-\mu)\pi}{2} - \mu\omega_c^{\mu-1}\cos\frac{(1-\mu)\pi}{2}$. In such a case, one can solve K_d and μ simultaneously utilizing Eqs. (11) and (13).

In view of specification (iii), the equation about K_p can be obtained as

$$|G(j\omega_c)| = \frac{K_p K\sqrt{(1 + K_d\omega_c^\mu\cos\frac{\mu\pi}{2})^2 + (K_d\omega_c^\mu\sin\frac{\mu\pi}{2})^2}}{\omega_c\sqrt{1 + (\omega_c T)^2}} = 1. \qquad (14)$$

In this way, the control gain K_p could be explicitly solved as

$$K_p = \frac{\omega_c\sqrt{1 + (\omega_c T)^2}}{K\sqrt{(1 + K_d\omega_c^\mu\cos\frac{\mu\pi}{2})^2 + (K_d\omega_c^\mu\sin\frac{\mu\pi}{2})^2}} \qquad (15)$$

3.2 FO (PD) Controller

The FO (PD) controller is designed in the form of [17]

$$C_2(s) = K_{p2}(1 + K_{d2}s)^{\mu} \tag{16}$$

which can be rewritten as

$$C_2(j\omega) = K_{p2}(1 + K_{d2}(j\omega))^{\mu} \tag{17}$$

In this way, the phase and gain of Eq. (17) are

$$\arg[C_2(j\omega)] = \mu\tan^{-1}(\omega K_{d2}),\ |C_2(j\omega)| = K_{p2}(1 + (K_{d2}\omega)^2)^{\frac{\mu}{2}} \tag{18}$$

The open-loop transfer function $G_2(s)$ is obtained as $G_2(s) = C_2(s)P(s)$. In this way, the phase and gain of $G_2(s)$ are

$$\arg[G_2(j\omega)] = \mu\tan^{-1}(\omega K_{d2}) - \tan^{-1}(\omega T) - \frac{\pi}{2} - \omega L \tag{19}$$

$$|G_2(j\omega)| = \frac{K_{p2}K(1 + (K_{d2}\omega)^2)^{\frac{\mu}{2}}}{\omega\sqrt{1 + (\omega T)^2}} \tag{20}$$

The parameter tunning for the FO (PD) controller, as well as the following controllers, is the same with the PD^{μ} controller. The meet the specification (i), the relationship between K_d and μ can be expressed as

$$K_{d2} = \frac{1}{\omega_c}\tan(\frac{1}{\mu}(\phi_m - \frac{\pi}{2} + \tan^{-1}(T\omega_c) + \omega_c L)) \tag{21}$$

To meet the specification (ii), the relationship between K_{d2} and μ can be expressed as

$$\omega_c^2 A K_{d2}^2 - \mu K_{d2} + A = 0 \Longrightarrow K_{d2} = \frac{\mu \pm \sqrt{\mu^2 - 4(A\omega_c)^2}}{2(A\omega_c)^2} \tag{22}$$

To meet the specification (iii), K_{p2} can be obtained as

$$K_{p2} = \frac{\omega_c\sqrt{(T\omega_c)^2 + 1}}{K(1 + (k_{d2}\omega_c)^2)^{\frac{\mu}{2}}} \tag{23}$$

3.3 PI^{λ} Controller

The PI^{λ} controller is designed in the form as follows [21]

$$C_3(s) = K_{p3}(1 + \frac{K_i}{s^{\lambda}}) \tag{24}$$

The phase and gain of Eq. (24) is

$$\arg[C_3(j\omega)] = -\tan^{-1}[\frac{K_i\omega^{-\lambda}\sin(\frac{\lambda\pi}{2})}{1 + K_i\omega^{-\lambda}\cos(\frac{\lambda\pi}{2})}] \tag{25}$$

$$|C_3(j\omega)| = K_p\sqrt{(1+K_i\omega^{-\lambda}\cos(\frac{\lambda\pi}{2}))^2+(K_i\omega^{-\lambda}\sin(\frac{\lambda\pi}{2}))^2} \tag{26}$$

The phase and gain of the open-loop transfer function are

$$\arg[G_3(j\omega)] = -\tan^{-1}[\frac{K_i\omega^{-\lambda}\sin(\frac{\lambda\pi}{2})}{1+K_i\omega^{-\lambda}\cos(\frac{\lambda\pi}{2})}] - \tan^{-1}(\omega T) - \frac{\pi}{2} - \omega L \tag{27}$$

$$|G_3(j\omega)| = \frac{KK_{p3}\sqrt{(1+K_i\omega^{-\lambda}\cos(\frac{\lambda\pi}{2}))^2+(K_i\omega^{-\lambda}\sin(\frac{\lambda\pi}{2}))^2}}{\omega\sqrt{\omega^2T^2+1}} \tag{28}$$

To satisfy the specification (i), one can obtain

$$\frac{K_i\omega_c^{-\lambda}\sin(\frac{\lambda\pi}{2})}{1+K_i\omega_c^{-\lambda}\cos(\frac{\lambda\pi}{2})} = \tan(\tan^{-1}(T\omega_c)+L\omega_c+\phi_m-\frac{\pi}{2}) \tag{29}$$

Then the relationship between K_i and λ can be established as

$$K_i = \frac{C}{\omega_c^{-\lambda}\sin(\frac{\lambda\pi}{2}) - C\omega_c^{-\lambda}\cos(\frac{\lambda\pi}{2})} \tag{30}$$

where $C = \tan(\tan^{-1}(T\omega_c)+L\omega_c+\phi_m-\frac{\pi}{2})$.

To satisfy the specification (ii), one can obtain

$$\frac{K_i\lambda\omega_c^{\lambda-1}\sin(\frac{\lambda\pi}{2})}{\omega_c^{2\lambda}+2K_i\omega_c^{\lambda}\cos(\frac{\lambda\pi}{2})+K_i^2} = A \Longrightarrow K_i = \frac{-F\pm\sqrt{F^2-4A^2\omega_c^{-2\lambda}}}{2A} \tag{31}$$

where $F = 2A\omega_c^{-\lambda}\cos(\lambda\pi/2) - \lambda\omega_c^{-\lambda-1}\sin(\lambda\pi/2)$.

To satisfy the specification (iii), one can obtain

$$K_{p3} = \frac{\omega_c\sqrt{\omega_c^2T^2+1}}{K\sqrt{(1+K_i\omega_c^{-\lambda}\cos(\frac{\lambda\pi}{2}))^2+(K_i\omega_c^{-\lambda}\sin(\frac{\lambda\pi}{2}))^2}} \tag{32}$$

3.4 FO (PI) Controller

The FO (PI) controller is designed in the form as follows [21]

$$C_4(s) = (K_{p4}+\frac{K_i}{s})^{\lambda} \tag{33}$$

The phase and gain of this controller is

$$\arg[C_4(j\omega)] = -\lambda\tan^{-1}(\frac{K_i}{K_{p4}\omega}),\ |C_4(j\omega)| = (K_{p4}^2+\frac{K_i^2}{w^2})^{\frac{\lambda}{2}} \tag{34}$$

The phase and gain of the open-loop $G_4(s)$ is

$$\arg[G_4(j\omega)] = -\lambda\tan^{-1}(\frac{K_i}{K_{p4}\omega}) - \tan^{-1}(\omega T) - \frac{\pi}{2} - L\omega \tag{35}$$

$$|G_4(j\omega)| = \frac{K(K_{p4}^2 + \frac{K_i^2}{\omega_c^2})^{\frac{\lambda}{2}}}{\omega\sqrt{1+(\omega T)^2}} \tag{36}$$

To satisfy the specification (i), one can obtain

$$\frac{K_i}{K_{p4}} = D = \omega_c \tan(-(\phi_m - \frac{\pi}{2} + \tan^{-1}(\omega_c T) + L\omega_c)/\lambda) \tag{37}$$

To satisfy the specification (ii), one can obtain

$$\frac{\lambda K_i K_{p4}}{(K_{p4}\omega_c)^2 + K_i^2} = A \tag{38}$$

To satisfy the specification (iii), one can obtain

$$K_{p4}^2 + \frac{K_i^2}{\omega_c^2} = E = (\frac{\omega_c}{K}\sqrt{1+(\omega_c T)^2})^{\frac{2}{\lambda}} \tag{39}$$

From Eqs. (37), (38) and (39), one can obtain

$$\lambda = A\frac{\omega_c^2 + D^2}{D},\ K_{p4} = \sqrt{\omega_c^2 E \omega_c^2 + D^2},\ K_i = K_{p4}D \tag{40}$$

4 Simulations

To verify the effectiveness of the developed FOCs for the quadrotor, extensive numeric simulations are conducted in this section.

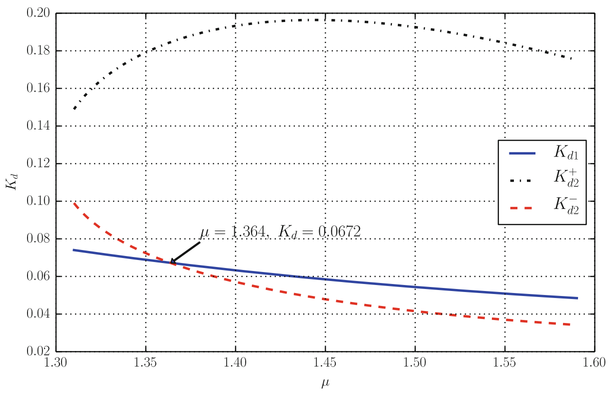

Fig. 2. The plot of K_d vs. μ.

To demonstrate the merits of the FOCs over their conventional counterparts, this work first investigates whether the PID controller could satisfy the specifications (i) to (iii). In view of Eqs. (9) and specification (ii), for a classic PD controller, one can obtain

$$\frac{\mathrm{d}(\arg[G(j\omega])}{\mathrm{d}\omega}|_{\omega=\omega_c} = \frac{K_d}{1+(K_d\omega_c)^2} - \frac{T}{1+(T\omega_c)^2} - L = 0 \tag{41}$$

The solution is $K_d = \frac{1\pm\sqrt{1-4\omega_c^2 A^2}}{2\omega_c^2 A}$, where $A = \frac{T}{1+(\omega_c T)^2} + L$. In such a case, the phase of $G(j\omega)$ is obtained as

$$\arg[G(j\omega_c)] = \tan^{-1}(K_d\omega_c) - \tan^{-1}(\omega_c T) - \frac{\pi}{2} - \omega_c L \tag{42}$$

This means $\arg[G(j\omega_c)]$ is a constant with determined K_d. As a result, specifications (i) and (ii) cannot be satisfied simultaneously for traditional PD controller.

In contrast, the parameters of the FOCs can be analytically solved with the aforementioned specifications. In this work, the PD^{μ} controller is adopted to demonstrate this feature, which is obviously the same with the other three kinds of FOCs. As formulated in Sect. 3, the PD^{μ} controller can be properly designed utilizing Eqs. (11), (13) and (15). By assigning $\phi_m = 70°$, $\omega_c = 5$, the parameters K_d and μ can be determined based on the graphic illustration. As shown in Fig. 2, the K_d and μ are explicitly determined as the intersection point, then K_p is evaluated by using Eq. (15). In this way, the control gains are determined as $K_d = 0.0672$, $\mu = 1.364$, and $K_p = 4.3$.

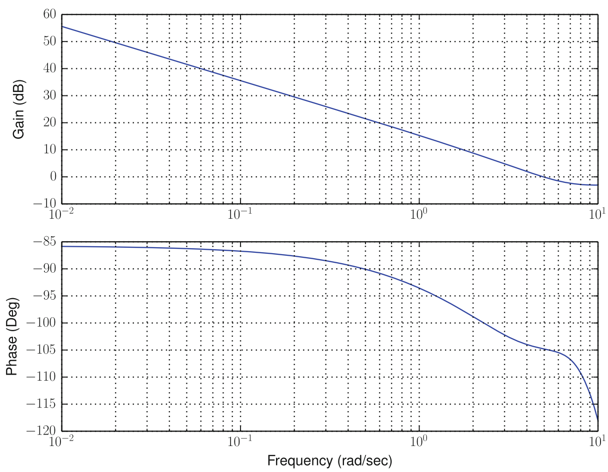

Fig. 3. The frequency response of open-loop plant with the PD^{μ} controller.

The bode plot of the corresponding controller is illustrated in Fig. 3. It can be seen that both the phase margin ϕ_m and the gain crossover frequency criterion ω_c (specification ii) are properly satisfied.

With the aforementioned parameters, the performance of the PD^{μ} controller is compared to the classic PD controller. The parameters of the conventional PID controller are selected by utilizing the ITAE criterion and the system Simulation techniques [22]. As the PD^{μ} is actually a finite dimensional linear filter due to the fractional order differentiator [20]. A band-limit implementation is important in practice, and a finite dimensional approximation method, namely Oustaloup Recursive Algorithm, is utilized in this work [20]. The comparative simulation results are illustrated in Fig. 4, where n is the order of the transfer function used in the approximation [20].

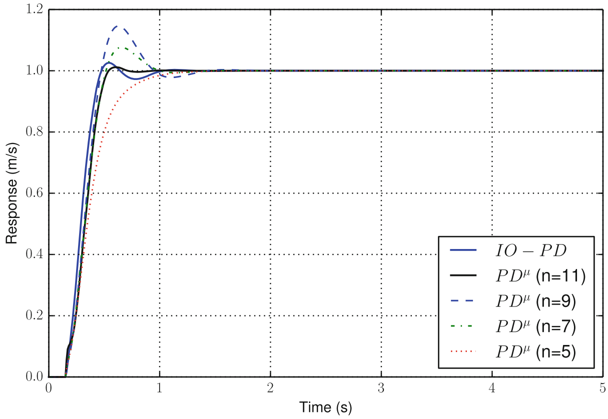

Fig. 4. The comparative simulation results of the PD^{μ} controller and the $IO-PD$ controller.

It can be seen that when the approximation order is relatively small, the performance of the FOC varies much. When n becomes larger, say $n = 11$, PD^{μ} controller demonstrates better stabilities as well as accuracy, thus shows its superiority over the traditional PD controller.

As an additional demonstration, the parameter tunning and step response of the PI^{λ} controller is illustrated in Fig. 5. With the proposed approach, the desired parameter can be effectively obtained as $K_p = 2.4$, $K_i = 0.32$, and $\mu = 0.202$.

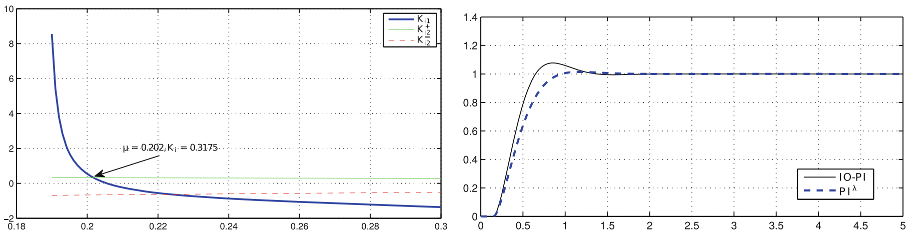

(a) Parameter tunning (b) Step response

Fig. 5. The comparative simulation results of the PI^{λ} controller and the $IO-PD$ controller.

With the tunned parameters, the response of the quadrotor compared to the PI controller is illustrated in Fig. 5(b). It can be seen that the PI^{λ} controller demonstrate faster convergence compared to the conventional PI controller.

5 Conclusion

This work has developed a class of FOCs and the associated parameter tunning methods for quadrotors, regarding the attitude as the pseudo control input. To facilitate this development, the transfer function of the attitude is first presented based on previous researches. With the obtained transfer function model, a class of FOCs, including PD^{μ}, FO(PD), PI^{λ}, and FO (PI) controllers are developed accordingly. For each controller, the parameter tunning methods are addressed in details. To verify the effectiveness of this development, comparative numeric simulations are carried out. The results show that with proper implementation, the FOCs demonstrate better robustness and stabilities over their conventional counterpart.

In future, the fractional calculus would be adopted to more accurately describe the quadrotor model, and the proposed controller is considered to implement into real-time flights to improve the performance of quadrotor in their specific missions.

Acknowledgments. This work was funded by the special development fund of Shanghai Zhangjiang Hi-Tech Industrial Development Zone (No. 201411-PD-JQ-B108-009) and Open Foundation of the State Key Laboratory of Fluid Power Transmission and Control (No. GZKF-201510).

References

1. Burri, M., Oleynikova, H., Achtelik, M., Siegwart, R.: Real-time visual-inertial mapping, re-localization and planning onboard MAVs in unknown environments. In: Proceedings of the IEEE/RSJ International Conference on Intelligent Robots and Systems, Hamburg, pp. 1872–1878, September 2015
2. Dong, W., Gu, G.Y., Ding, Y., Xiangyang, Z., Ding, H.: Ball juggling with an under-actuated flying robot. In: Proceedings of the IEEE/RSJ International Conference on Intelligent Robots and Systems, Hamburg, pp. 68–73, September 2015
3. Hehn, M., D'Andrea, R.: A flying inverted pendulum. In: Proceedings of IEEE International Conference on Robotics and Automation, pp. 763–770 (2011)
4. Kumar, V., Michael, N.: Opportunities and challenges with autonomous micro aerial vehicles. Int. J. Robot. Res. **31**(11), 1279–1291 (2012)
5. Bouabdallah, S., Noth, A., Siegwart, R.: PID vs LQ control techniques applied to an indoor micro quadrotor. IN: Proceedings of the IEEE/RSJ International Conference on Intelligent Robots and Systems, vol. 3, pp. 2451–2456 (2004)
6. Droeschel, D., Nieuwenhuisen, M., Beul, M., Holz, D., Stückler, J., Behnke, S.: Multilayered mapping and navigation for autonomous micro aerial vehicles. J. Field Robot. (2015). doi:10.1002/rob.21603. Article first published online: 5 June 2015

7. Dydek, Z.T., Annaswamy, A.M., Lavretsky, E.: Adaptive control of quadrotor UAVs: a design trade study with flight evaluations. IEEE Trans. Autom. Sci. Eng. **21**, 1400–1406 (2013)
8. Mellinger, D., Kumar, V.: Minimum snap trajectory generation and control for quadrotors. In: Proceedings of IEEE International Conference on Robotics and Automation, pp. 2520–2525 (2011)
9. Richter, C., Bry, A., Roy, N.: Polynomial trajectory planning for aggressive quadrotor flight in dense indoor environments. In: Proceedings of the International Symposium on Robotics Research, Singapore, 1–16 December 2013
10. Bouabdallah, S.: Design and control of quadrotors with application to autonomous flying. Ph.D. thesis (2007)
11. Ryan, T., Kim, H.: Lmi-based gain synthesis for simple robust quadrotor control. IEEE Trans. Autom. Sci. Eng. **10**(4), 1173–1178 (2013)
12. Dong, W., Gu, G.Y., Zhu, X., Ding, H.: High-performance trajectory tracking control of a quadrotor with disturbance observer. Sens. Actuators A Phys. **211**, 67–77 (2014)
13. Lim, H., Park, J., Lee, D., Kim, H.: Build your own quadrotor: open-source projects on unmanned aerial vehicles. IEEE Robot. Autom. Mag. **19**(3), 33–45 (2012)
14. Michael, N., Mellinger, D., Lindsey, Q., Kumar, V.: The grasp multiple micro-UAV testbed. IEEE Robot. Autom. Mag. **17**(3), 56–65 (2010)
15. Peng, C., Tian, Y., Bai, Y., Gong, X., Zhao, C., Gao, Q., Xu, D.: ADRC trajectory tracking control based on PSO algorithm for a quad-rotor. In: Proceedings of the IEEE Conference on Industrial Electronics and Applications, pp. 800–805 (2013)
16. Podlubny, I.: Fractional-order systems and pi/sup/spl lambda//d/sup/spl mu//-controllers. IEEE Trans. Autom. Control **44**(1), 208–214 (1999)
17. Luo, Y., Chen, Y.: Fractional order [proportional derivative] controller for a class of fractional order systems. Automatica **45**(10), 2446–2450 (2009)
18. Dong, W., Gu, G., Zhu, X., Ding, H.: Modeling and control of a quadrotor UAV with aerodynamic concepts. In: ICIUS 2013: International Conference on Intelligent Unmanned Systems (2013)
19. Palka, B.: An Introduction to Complex Function Theory. Undergraduate Texts in Mathematics. Springer, London (2012)
20. Li, H., Luo, Y., Chen, Y.Q.: A fractional order proportional and derivative (FOPD) motion controller: tuning rule and experiments. IEEE Trans. Control Syst. Technol. **18**(2), 516–520 (2010)
21. Malek, H., Luo, Y., Chen, Y.: Identification and tuning fractional order proportional integral controllers for time delayed systems with a fractional pole. Mechatronics **23**(7), 746–754 (2013)
22. Chen, Y., et al.: System Simulation Techniques with MATLAB and Simulink. Wiley, London (2013)